Springer

KSME

Journal of Mechanical Science and Technology 25 (3) (2011) 827~836
www.springerlink.com/content/1738-494x
DOI 10.1007/s12206-011-0110-z

Temperature and thickness effects on thermal and mechanical stresses of rotating FG-disks †

Mehrnoosh Damircheli[1] and Mohammad Azadi[2,*]

[1]*Shahre-Qods Branch, Islamic Azad University, Tehran, Iran*
[2]*Mechanical Engineering Department, Sharif University of Technology, Tehran, Iran*

(Manuscript Received July 25, 2010; Revised October 22, 2010; Accepted November 22, 2010)

Abstract

In the present paper, radial and hoop thermal and mechanical stress analysis of a rotating disk made of functionally graded material (FGM) with variable thickness is carried out by using finite element method (FEM). To model the disk by FEM, one-dimensional two-degree elements with three nodes are used. It is assumed that the material properties, such as elastic modulus, Poisson's ratio and thermal expansion coefficient, are considered to vary using a power law function in the radial direction. The geometrical and boundary conditions are in the shape of two models including thermal stress (model-A) and mechanical stress (model-B). In model-A there exists no pressure in both external and internal layers, and there is a temperature distribution considered as a second order function in the radial direction of the rotating disk. In this case, the temperature dependency of the material properties is considered and a hyperbolic type is assumed for the geometry of the disk. In model-B, there is a constant pressure only on the internal layer and a pressure on the internal layer of the disk without temperature distribution but with different types of surface profiles. Furthermore, the displacements and stresses for various power law indices (N) and angular velocities are calculated and compared to other results in the literature. The effect of varying thicknesses and dependency of material properties on temperature distribution is investigated.

Keywords: Finite element method; Functional graded material; Rotating disk; Variable thickness; Temperature dependency

1. Introduction

Recent research on new applicable materials known as functionally graded materials (FGMs) illustrate that these materials have a good capability for resisting high temperatures and also severe temperature gradients. The concept of FGM was proposed in 1984 by a group of materials scientists in Sendai, Japan. These materials are appropriate for space structures, aircraft bodies and nuclear fusion reactors [1]. In developing FGMs, a lot of work has been performed on this topic. A recent paper by You et al. [2] discusses deformations and stresses in annular disks made of functionally graded materials subjected to internal and/or external pressure The main process of this development, however, began in 1995 [3, 4].

FGMs are a combination of different materials, including metals and ceramics. They are non-homogeneous on a microscopic scale and completely different from composites materials due to their continuously changing microscopic properties [5]. Usually, these changes are related to material parameters and are considered as power or exponential functions in the radius or thickness directions of the disk. Rotating disks play a vital role in turbo machines and flywheels of automobiles. Usually, for simplicity in analyzing rotating disks, plane strain or plane stress assumptions are used. In this paper, the plane stress state is considered [6-10]. A lot of research has been presented on the stress analysis of FGMs, including some of our recent works [11-13]. Some of these papers are related to rotating FG disks.

Leissa and Vagins [14] and Jain et al. [15] optimized the distribution of stresses in rotating disks by varying elastic coefficient as a function of radius. Jain et al. [16] and Zhou and Ogawa [17] presented an analytical method for analyzing rotating disks. In their investigation, the elastic coefficient was considered a function of circumferential coordinates. Ramu and Iyengar [18] studied the effect of longitudinal stress on internal plane stresses and stated the quasi-three dimensional elastic stresses in rotating disks. Chen and Lee [19] considered the problem of a simply-supported, laminated orthotropic, rotating cylindrical shell by involving centrifugal forces as well as the Coriolis acceleration effect. Mian and Spencer [20] studied the deformation of symmetric rotating disks made of FGMs. In this study, elastic coefficient was considered to be a function of the disk's thickness. Chen et al. [21] derived an analytical solution for rotating disks made of FGMs. In their

† This paper was recommended for publication in revised form by Editor Maenghyo Cho

*Corresponding author. Tel.: +98 910 2107280, Fax.: +98 21 22201301
E-mail address: azadi@mech.sharif.ir, m.azadi.1983@gmail.com

investigation, all material properties were considered to vary in the thickness direction of the disk, and optimization was carried out according to the distribution of radial and hoop stresses. Zenkour [22] calculated the stress distributions in FGM disks with an accurate elastic solution for exponentially graded rotating angular disks with constant thickness. Bayat et al. [23] considered the analysis of functionally graded rotating disks with variable thickness. In another paper, Bayat et al. [24] performed a thermoelastic solution of a functionally graded, variable thickness rotating disk with bending based on the first-order shear deformation theory. Chen et al. [25] considered a three-dimensional analytical solution for a rotating disc of functionally graded materials with transverse isotropy.

In almost all of the previously mentioned research, the temperature dependency of material properties and thickness variation of rotating disks are neglected. Therefore, in the present paper, stress analysis of a rotating disk made of FGMs is conducted by using finite element method (FEM) and considering the effect of thickness variation and dependency of material properties to temperature distribution. The properties of the disk are considered as power law functions of radius. These properties include elastic modulus, Poisson's ratio and thermal expansion coefficient. Two models are considered for geometrical and boundary conditions including thermal (model-A) and mechanical (model-B) stresses. In model-A, temperature dependency of the properties of this disk is also considered. The displacements and stresses for various power law indices and angular velocities are studied in the radius direction.

2. Governing equation

2.1 Material modeling

FGMs are a combination of metals and ceramics. They can be used in high temperature conditions, so their properties are dependent on temperature. Constitutional properties of metals and ceramics should be stated as functions of temperature; these properties include elastic modulus, Poisson's ratio, thermal conductivity coefficient, thermal expansion coefficient and thermal capacity as follows [26]:

$$P(T) = P_0\left(P_{-1}T^{-1} + 1 + P_1T + P_2T^2 + P_3T^3\right) \tag{1}$$

where P_i (i = -1, 0, 1, 2, 3) are constants of the aforementioned properties and T is temperature. Volume fraction is a spatial function, whereas properties of constituents are functions of temperature. Combining these functions gives rise to effective material properties (P_{eff}) of FGMs according to temperature (T) and disk radius (r) as follows:

$$P_{eff}(T,r) = P_m(T)V_m(r) + P_c(T)V_c(r) \tag{2}$$

in which, P_{eff} is effective material property and P_m and P_c are the temperature-dependent properties of metal and ceramic, respectively. V_c and V_m are volume fractions of ceramic and metal constituent which have a relation as follows:

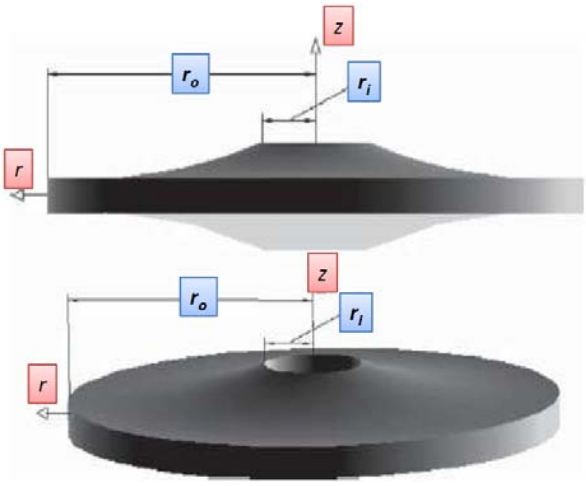

Fig. 1. Schematic of an FG disk with variable thickness.

$$V_m(r) + V_c(r) = 1\,. \tag{3}$$

Volume fractions can be presented in different forms. In this study, volume fraction is considered according to Reddy's assumption [26] as follows:

$$V_j(r) = \left(\frac{r - r_i}{r_o - r_i}\right)^N \quad : j \equiv c,m \tag{4}$$

in which r_i is inner radius and r_o is outer radius of the disk, and N (power law index) is a material constant whose value can change from zero to infinity.

2.2 Structural modeling

There are many cases in engineering practice, such as for rotating disks, that the distribution of stresses about one axis could be symmetrical. Such cases can be considered as in plane stress state (σ_z = 0) and displacement is not related to circumferential coordinate (θ) but is only a function of radius (r). Moreover, due to symmetry, the shear stress is zero, while the radial and hoop stresses are non-zero.

In a rotating disk with constant thickness, the maximum stress will appear on internal layers. Therefore, to reduce weight and the effect of centrifugal force, in many designs of disks, such as that of steam turbines, the internal layers are usually thicker in comparison to external layers. Also, in the design of such disks, a smooth distribution of stresses is preferred (especially hoop stress). To obtain this purpose, the material distribution can be changed.

A schematic of an FG disk with variable thickness is shown in Fig. 1.

Analysis of the disk with variable thickness is similar to the disk with constant thickness. For this case, two types of profiles are considered.

Model-A) The profile of the radial section assumed to be of

Table 1. The geometrical parameters of the FG disk in model-A.

Characteristic	Contents
Inner Radius (r_i)	0.05000 (m)
Outer Radius (r_o)	0.25000 (m)
Inner Height (h_i)	0.07500 (m)
Outer Height (h_o)	0.01500 (m)
Hyperbolic Constant (h_1)	0.00375 (m)
Hyperbolic Constant (p)	1.000000 (-)

Table 2. Constants of geometric model of the disk in model-B.

Structure type	*m*	*q*
a (Concave)	0.5	0.96
b (Linear)	1.0	0.80
c (Convex)	3.0	0.42
d (Constant thickness)	-	0.00

hyperbolic type:

$$h(r) = h_1 r^{-s} \quad . \tag{5a}$$

In the above equation, h_1 and p are constants and p is positive definite. Furthermore, h_1 is the thickness in section with unit radius. This assumption is not appropriate for solid rotation disks, because at the center of the disk (r = 0), the thickness approaches infinity. The geometrical parameters of this model are listed in Table 1.

Model-B) The profile of the radial section assumed to be as a power law:

$$h(r) = h_o\left[1 - q\left(\frac{r}{r_o}\right)^m\right] \tag{5b}$$

in which h_0, q and m are constants listed in Table 2.

The differential equation in this case is as follows [27, 30]:

$$\frac{d}{dr}\left(h(r)\sigma_r\right) - \frac{h(r)}{r}\left(\sigma_r - \sigma_\theta\right) + h(r)\rho(r)r\omega^2 = 0 \tag{6}$$

in which σ_r, σ_θ, ω and ρ are hoop stress, radial stress, angular velocity and volume density, respectively. In this paper, the effect of volume weight force is neglected. In a rotating disk, the stresses are functions of strains as follows [27, 30]:

$$\sigma_r = \frac{E(r)}{1-v^2}\left(\varepsilon_r + v\varepsilon_\theta - (1+v)\alpha\Delta T\right) \tag{7a}$$

$$\sigma_\theta = \frac{E(r)}{1-v^2}\left(\varepsilon_\theta + v\varepsilon_r - (1+v)\alpha\Delta T\right) \tag{7b}$$

where α, ΔT, E and v are thermal expansion coefficient, temperature difference, elastic modulus and Poison's ratio, respectively. In the present paper, elastic modulus is considered as change in different radius and Poison's ratio is considered as a constant. The relations between strains and deformations are described as follows:

$$\varepsilon_r = \frac{du}{dr}, \quad \varepsilon_\theta = \frac{u}{r} \quad . \tag{8}$$

Therefore, the differential equation of a rotating disk can be obtained as follows:

$$\begin{aligned}&\frac{d}{dr}\left[\frac{h(r)E(r)}{1-v^2}\left(\frac{du}{dr} + v\frac{u}{r} - (1+v)\alpha\Delta T\right)\right] + \\ &\frac{h(r)E(r)}{r(1+v)}\left(\frac{u}{r} - \frac{du}{dr}\right) + h(r)\rho(r)r\omega^2 = 0.\end{aligned} \tag{9}$$

The above relation is the governing equation.

3. Finite element method (FEM)

To solve the governing equation for the FG disk, the finite element method (FEM) is used. According to this procedure, the Kantorovich approximation is considered as follows [28-29].

$$u(r,t) = \left[N(r)\right]\left\{U(t)^{(e)}\right\} \quad : e = 1,...,n \tag{10a}$$

in which e and n are element number and the number of elements, respectively. $[N(r)]$ is shape function matrix for two degree elements (with 3 nodes) and can be written as follows [28-29]:

$$\left[N(r)\right] = \left[\frac{1}{2}\xi(\xi-1),\ \left(1-\xi^2\right),\ \frac{1}{2}\xi(\xi+1)\right] \tag{10b}$$

where ξ is natural coordinate and its value varies between -1 and 1 content. The reason for employing this coordinate is in order to use the Gauss-Legendre numerical integration method. The integration form of whole volume (V) of disks in the Galerkin method is shown below:

$$\int_V \left[N\right]^T R dV = 0 \tag{11a}$$

where

$$\begin{aligned}R = &\frac{d}{dr}\left[\frac{h(r)E(r)}{1-v^2}\left(\frac{du}{dr} + v\frac{u}{r} - (1+v)\alpha\Delta T\right)\right] + \\ &\frac{h(r)E(r)}{r(1+v)}\left(\frac{u}{r} - \frac{du}{dr}\right) + h(r)\rho(r)r\omega^2\end{aligned} \tag{11b}$$

The above equation is then simplified to the following equa-

tion:

$$\left[K^{(e)}\right]\left\{U^{(e)}\right\}=\left\{f^{(e)}\right\} \tag{12a}$$

in which

$$\begin{aligned}\left[K^{(e)}\right]&=\int_V[N]^T\left\{\frac{d}{dr}\left[\frac{h(r)E(r)}{1-v^2}\left([N]_{,r}+\frac{v}{r}[N]\right)\right]\right\}dV\\&+\int_V[N]^T\left\{\frac{h(r)E(r)}{r(1+v)}\left(\frac{1}{r}[N]-[N]_{,r}\right)\right\}dV\\\left\{f^{(e)}\right\}&=\int_V\left\{\frac{d}{dr}\left[\frac{h(r)E(r)\alpha\Delta T}{1+v}\right]-h(r)\rho(r)r\omega^2\right\}[N]^T\,dV.\end{aligned} \tag{12b}$$

The displacement vector can be obtained from the above relation and then strain and stress can be calculated.

4. Boundary conditions

The stress boundary conditions, such as the aforementioned geometrical conditions, are assumed in two models including thermal (model-A) and mechanical (model-B) stress.

Model-A) Non-existence of radial pressure (consequently, zero radial stress) at both internal and external layers (inner and outer radius) of disk:

$$\begin{aligned}&r=r_i:\sigma_r=0\\&r=r_o:\sigma_r=0\end{aligned}\quad. \tag{13}$$

To satisfy the above conditions, Eq. (7a) can be written in the following form:

$$\begin{aligned}\sigma_r&=\left[B^{(e)}\right]\left\{U^{(e)}\right\}+\left\{C^{(e)}\right\}\\\left[B^{(e)}\right]&=\frac{E(r)}{1-v^2}\left([N]_{,r}+\frac{v}{r}[N]\right)\\\left\{C^{(e)}\right\}&=-\frac{E\alpha\Delta T}{1+v}\end{aligned}\quad. \tag{14}$$

Substituting the value of radial stress as zero in the first and last elements of the disk in Eq. (12a) simplifies the equation as follows:

$$\begin{aligned}&\left[K^{(e)}\right]_{n\times n}\left\{U^{(e)}\right\}_{n\times1}=\left\{f^{(e)}\right\}_{n\times1}\rightarrow\\&\begin{bmatrix}\left[B^{(1)}\right]&[0...0]&[0\ \ 0\ \ 0]\\[0\ \ 0\ \ 0]&\left[\tilde{K}^{(e)}\right]&[0\ \ 0\ \ 0]\\[0\ \ 0\ \ 0]&[0...0]&\left[B^{(n)}\right]\end{bmatrix}\begin{Bmatrix}\left\{U^{(1)}\right\}\\\left\{\tilde{U}^{(e)}\right\}\\\left\{U^{(n)}\right\}\end{Bmatrix}=\begin{Bmatrix}-\left\{C^{(1)}\right\}\\\left\{\tilde{f}^{(e)}\right\}\\-\left\{C^{(n)}\right\}\end{Bmatrix}\end{aligned}\quad. \tag{15}$$

In this model, the temperature distribution is considered as follows:

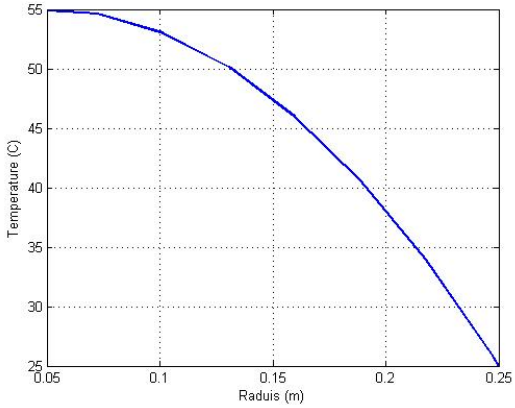

Fig. 2. Temperature distribution on the FG disk in model-A.

$$\Delta T=\left(T_2-T_1\right)\left(\frac{r-r_i}{r_o-r_i}\right)^2 \tag{16}$$

in which T_1 is 55℃ and T_2 is 25℃.

Model-B) Non-existence of radial pressure (consequently, zero radial stress) at internal (inner radius) and p_i on the external layers (outer radius) of disk:

$$\begin{aligned}&r=r_i:\sigma_r=-p_i\\&r=r_o:\sigma_r=0\end{aligned}\quad. \tag{17}$$

In this model, the temperature distribution is neglected and only mechanical stresses are considered. As a result, Eq. (15) is changed as follows:

$$\begin{aligned}&\left[K^{(e)}\right]_{n\times n}\left\{U^{(e)}\right\}_{n\times1}=\left\{f^{(e)}\right\}_{n\times1}\rightarrow\\&\begin{bmatrix}\left[B^{(1)}\right]&[0...0]&[0\ \ 0\ \ 0]\\[0\ \ 0\ \ 0]&\left[\tilde{K}^{(e)}\right]&[0\ \ 0\ \ 0]\\[0\ \ 0\ \ 0]&[0...0]&\left[B^{(n)}\right]\end{bmatrix}\begin{Bmatrix}\left\{U^{(1)}\right\}\\\left\{\tilde{U}^{(e)}\right\}\\\left\{U^{(n)}\right\}\end{Bmatrix}=\begin{Bmatrix}-p_i\\\left\{\tilde{f}^{(e)}\right\}\\0\end{Bmatrix}\end{aligned}\quad. \tag{18}$$

To solve these relations, a computer code is prepared in MATLAB software.

5. Numerical results

To show the distribution of displacement and stresses of the FG disk, two numerical examples are solved, including model-A and model-B.

5.1 Results for model-A

Here the angular velocity is 900 rpm and temperature distribution in the radius direction of the disk is shown in Fig. 2. The profile of the disk surface is shown in Fig. 3.

In this case, stainless steel and zirconium are used as the metal and ceramic constituents, respectively. The material

Table 3. The material properties of the FG disk in model-A.

Parameters	Metal (Stainless Steel)	Ceramic (Zirconium)
ρ (Kg/m^3)	7800	5700
E (GPa)	201.04	244.27
v	0.326	0.288
α (10^{-5}/K)	1.233	1.277
P_{-1} (E,α)	0	0
P_1 (E)	+3.079 X 10^{-4}	-1.371 X 10^{-3}
P_2 (E)	-6.530 X 10^{-8}	+1.214 X 10^{-6}
P_3 (E)	0	-3.680 X 10^{-10}
P_1 (α)	+8.086 X 10^{-4}	-1.490 X 10^{-3}
P_2 (α)	0	+1.000 X 10^{-6}
P_3 (α)	0	+6.800 X 10^{-12}

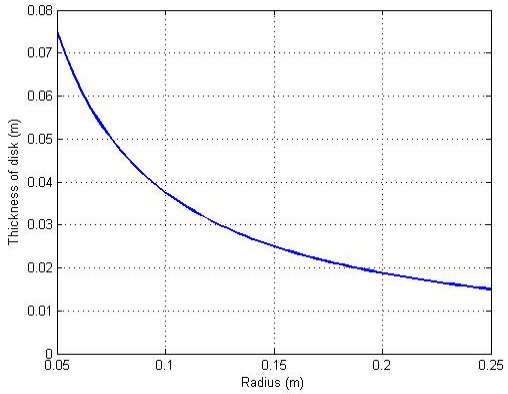

Fig. 3. Profile of the FG disk surface in model-A.

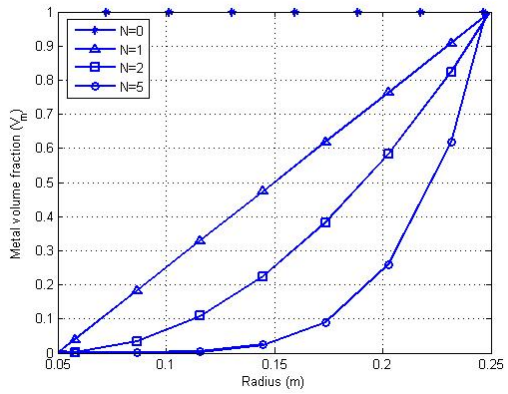

Fig. 4. Metal volume fraction for various *N*s in model-A.

properties of the rotating disk are mentioned in Table 3. The value of N for ceramic and metal-rich materials is infinity and zero, respectively. The external layer of the disk is metal-rich and the internal layer of disk is ceramic-rich. The metal volume fraction is drawn versus N and is shown in Fig. 4.

The radial displacement for different numbers of elements (n) (when $N = 0$), which is evidence for the convergence of the results, is shown in Fig. 5. Thus, 30 elements are chosen for further analysis.

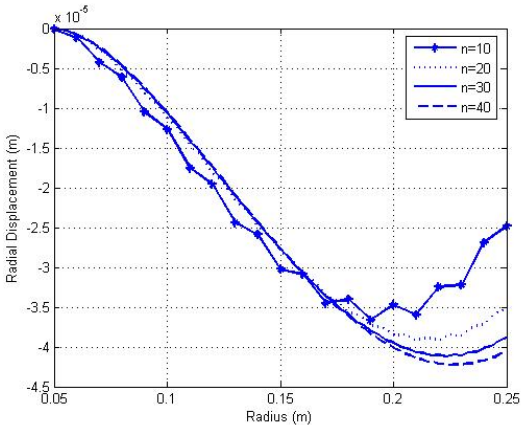

Fig. 5. Radial displacement for different numbers of elements (n) in model-A.

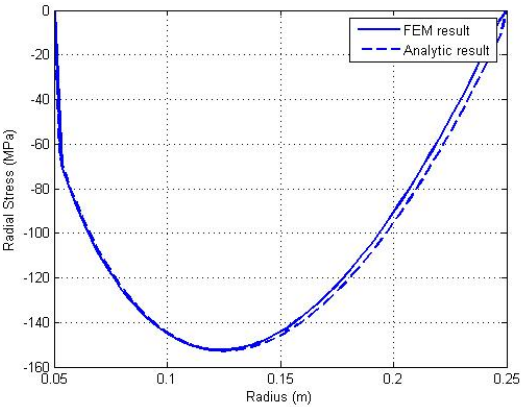

Fig. 6. Radial stress obtained by FEM and analytical method for $N = 0$ (metal-rich) in model-A.

When N is zero, the material properties are isotropic (metal-rich), and therefore, the governing differential equation of the rotating disk is reduced to the simplified governing equation for isotropic rotating disks given by Timoshenko [5] and can be solved by an analytical procedure. Fig. 6 shows the results of the present method and are compared to the results obtained by Ref. [5] for a stainless steel rotating disk with the material properties given in Table 4. The variation of radial stress obtained by both methods is compared for validation and confirms that there is good agreement between the results.

The effect of the angular velocity of the FG disk on the radial stress, hoop stress and radial displacement of rotating disk is shown in Figs. 7-9. As expected, increasing the angular velocity increases the radial, hoop stress and radial displacement. The maximum discrepancy in stresses occurs at the center of the disk's radius. In Table 4, the effect of angular velocity and power law index on the maximum radial stress has been investigated. As expected, increasing the magnitude of two parameters also increases the maximum radial stress in the rotating disk.

Table 4. Max Radial stress for Hoop stress for various angular velocity and N in model-A.

Angular Velocity (rpm)	Max Radial stress (Mpa)				
	N = 1	*N = 2*	*N = 3*	*N = 4*	*N = 5*
200	-70.3	-70.5	-70.6	-70.7	-70.9
500	-83.6	-89.1	-93.5	-95.2	-95.3
700	-94.7	-116.3	-126.3	-129.4	-129.5
1000	-128.3	-176.9	-198.6	-204.2	-204.7
1500	-206.4	-327.1	-377.7	-380.2	-390.4

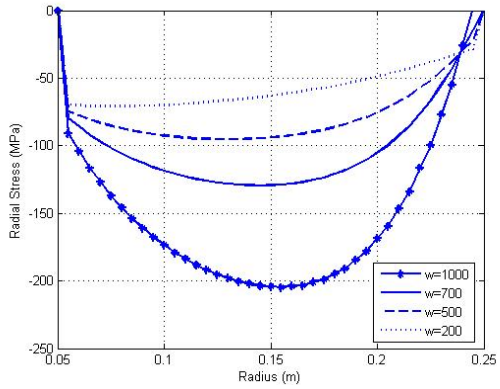

Fig. 7. Radial stress for various angular velocity and $N = 5$ in model-A.

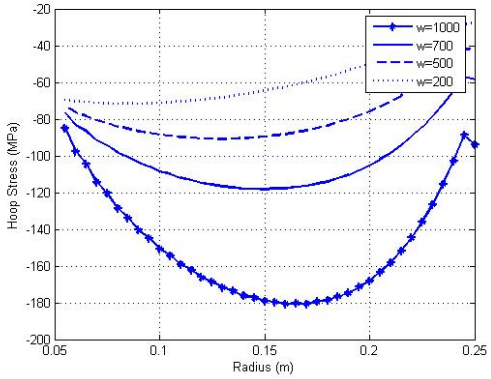

Fig. 8. Hoop stress for various angular velocity and $N = 5$ in model-A.

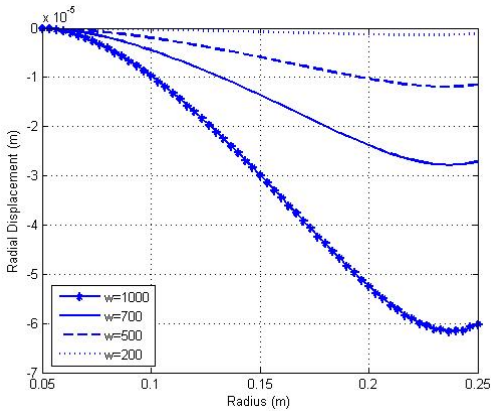

Fig. 9. Radial displacement for various angular velocity and $N = 5$ in model-A.

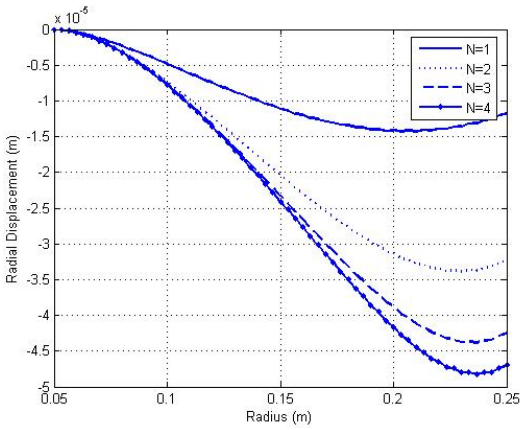

Fig. 10. Radial displacement for various *N*s in model-A.

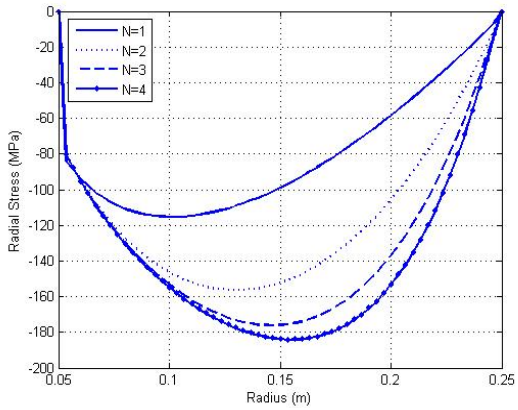

Fig. 11. Radial stress for various *N*s in model-A.

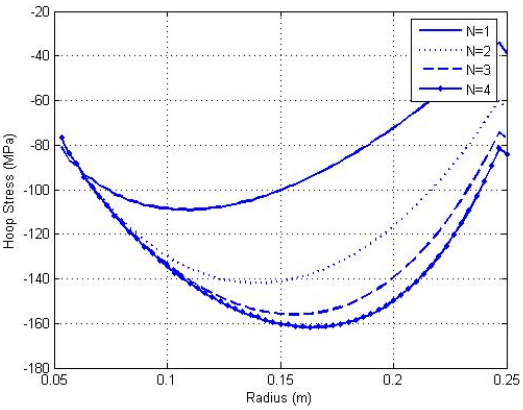

Fig. 12. Hoop stress for various *N*s in model-A.

The radial displacement, radial stress and hoop stress for various power law indices N along the radial direction is illustrated in Figs. 10-12. It should be mentioned that there is a small error near the boundary conditions due to numerical calculations.

Increasing the magnitude of N increases the displacement, and therefore, the stresses are also increased. It should be mentioned that the location of the maximum radial and hoop stresses (peak of the curves) in Figs. 11 and 12 is moved from

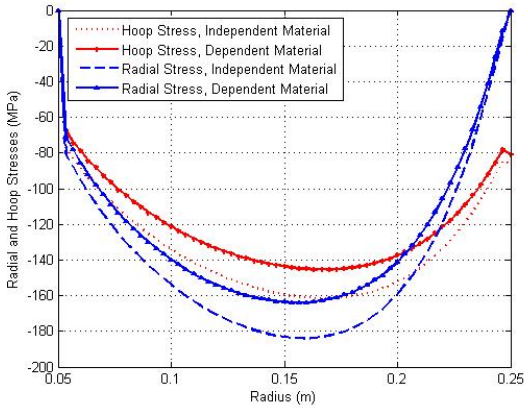

Fig. 13. Temperature dependency on radial and hoop stresses for $N = 5$ in model-A.

the internal layer to the external layer of the FG disk. The internal layer of the FG disk is ceramic-rich and its external layer is metal-rich. Therefore, by increasing N, the harder internal layer deflects to some extent, but the softer external layer is displaced more than the internal layer. Therefore, as shown in Fig. 10, by moving from the internal layer to the external layer, the displacement is increased.

In Eq. (2), the function of properties P, consists of two parts, namely temperature and location. If the temperature part is considered to be constant or the effect of temperature is neglected in the properties variation, Eq. (2) can be a function of location only and independent of temperature. To study the effect of temperature dependency of material properties on the response of the FG disk, the radial and hoop stress variations in two states of temperature-independent and temperature-dependent material properties along the radial direction for $N = 5$ are shown in Fig. 13.

The results show that temperature dependency is not a dismissible parameter due to a significant discrepancy (about 15%), which is remarkable in the values of radial and hoop stresses in rotating FG disks. Thus, the dependency of the material properties on temperature must be imposed in the design procedures.

5.2 Results for model-B

In this case, in inner radius of the disk is 0.2 m. Here, the angular velocity is 50 rad/sec, the internal pressure is 100 MPa and temperature distribution is neglected. The profiles of the disk surface are shown in Fig. 14. The material properties of the rotating disk are mentioned in Table 5. The external layer of the disk is ceramic-rich and the internal layer of the disk is metal-rich. The elastic modulus is drawn versus N and is shown in Fig. 15.

The non-dimensional radius and radial and hoop stresses are defined as follows:

$$\tilde{r} = \frac{r}{r_o}, \quad \tilde{\sigma}_r = \frac{\sigma_r}{p_i}, \quad \tilde{\sigma}_\theta = \frac{\sigma_\theta}{p_i}$$

Table 5. Material properties of the FG disk in model-B.

Properties	$r = r_i$ (Aluminum)	$r = r_o$ (Ceramic)
Young modulus (GPa)	70	151
Poison ratio	0.3	0.3
Density (Kg/m^3)	2700	5700

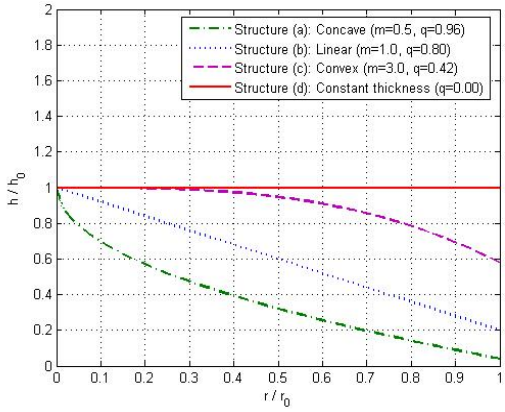

Fig. 14. Changing thickness of an FG disk for different profiles in model-B.

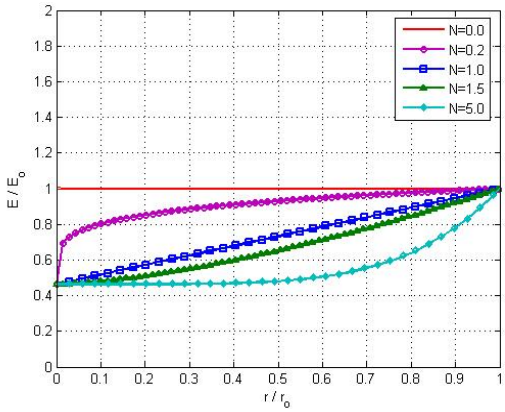

Fig. 15. Distribution of elastic modulus in model-B.

First, the convergence of the results is examined for different numbers of elements, n (Fig. 16). Then, 30 elements are used for further analysis.

To validate the code in this case, the present results are compared to Ref. [2]. For this case, an internal pressure (100 MPa) is applied on a non-rotating disk with a constant thickness. The inner and outer radiuses are 0.3 m and 0.5 m. Elastic modulus is considered 440 GPa in the inner layer and 110 GPa in the outer layer of the disk. The material properties are changed as linear relations ($N = 1$). The results are shown in Fig. 17 which has a good adoption.

The other results are shown in Figs. 18 and 19 ($N = 1$) and Figs. 20 and 21 ($N = 5$) for different disk profiles. In profile type (a), due to thickness reduction near the outer layer of the disk and constant applied internal pressure, force should de-

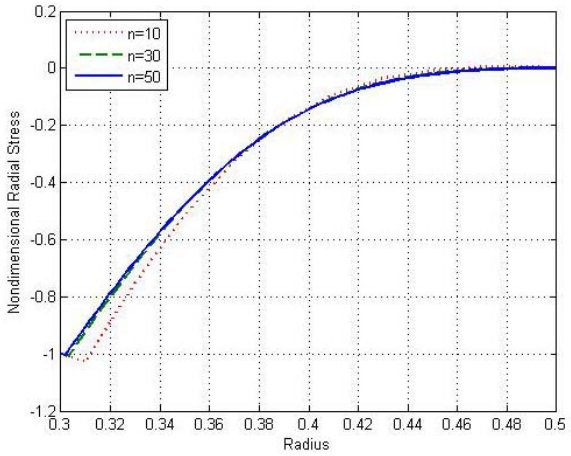

Fig. 16. Convergence of results for different numbers of elements (n) in model-B.

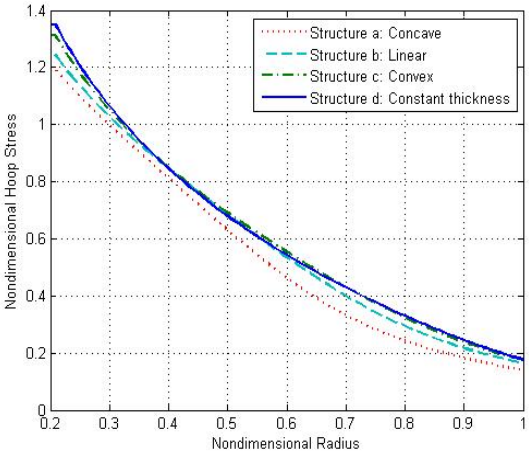

Fig. 19. Non-dimensional hoop stress versus non-dimensional radius for N=1 in model-B.

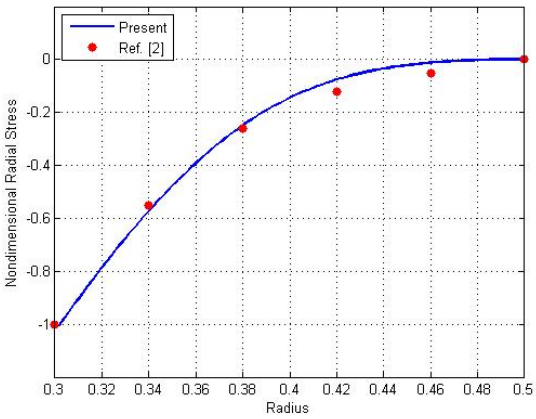

Fig. 17. Validation results of model-B in comparison to Ref. [2].

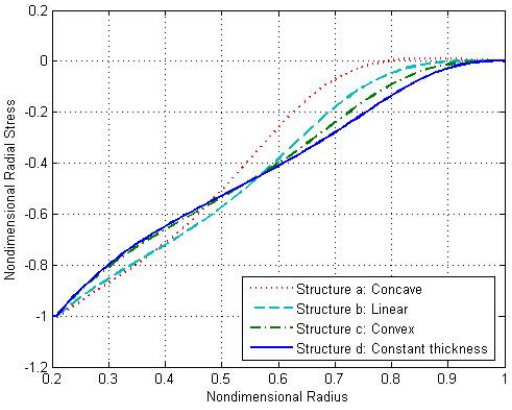

Fig. 20. Non-dimensional radial stress versus non-dimensional radius for N=5 in model-B.

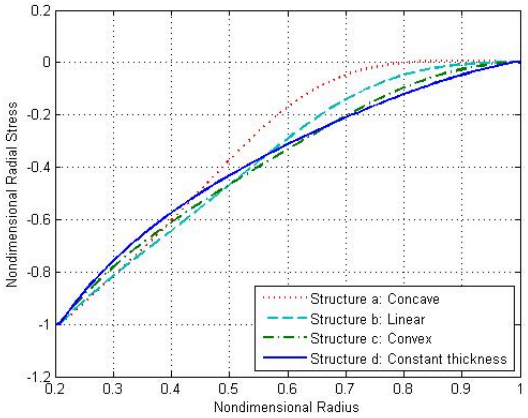

Fig. 18. Non-dimensional radial stress versus non-dimensional radius for N=1 in model-B.

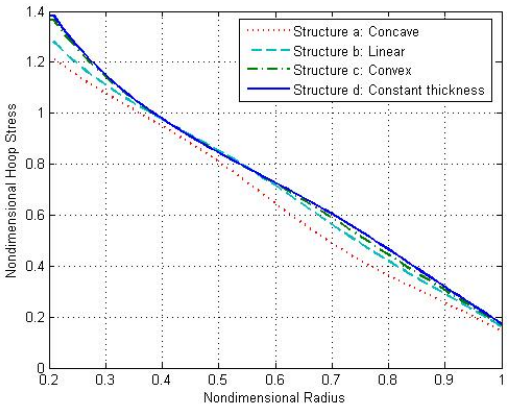

Fig. 21. Non-dimensional hoop stress versus non-dimensional radius for N=5 in model-B.

crease relative to the cross section of the disk, thus reducing radial stress in this area as well. This behavior is also seen for hoop stress (Fig. 19) in both different contents of N (Figs. 20 and 21).

In Figs. 22 and 23, radial and hoop stresses are drawn for different Ns in a disk with a constant thickness. In this model, zero content of N indicates a ceramic-rich material. By increasing N, the material properties almost become metal properties. As the material properties change, the stress behavior becomes complex.

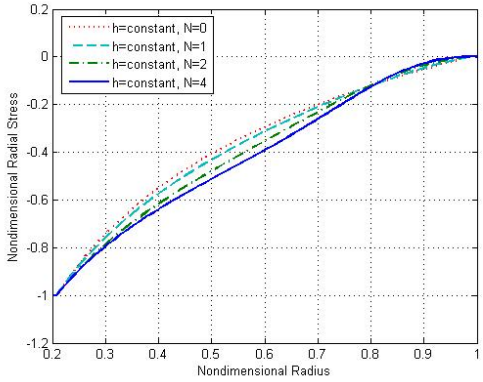

Fig. 22. Non-dimensional radial stress for a disk with constant thickness and different Ns in model-B.

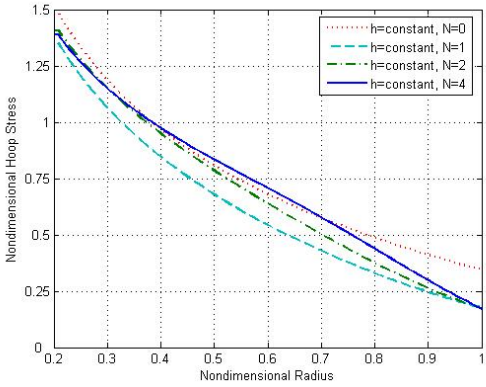

Fig. 23. Non-dimensional hoop stress for a disk with constant thickness and different Ns in model-B.

6. Conclusion

In the present paper, thermal and mechanical stresses of rotating FG disks are analyzed by FEM in two models of geometry and boundary conditions. The geometry of the disk in the direction of its thickness is variable and temperature dependency of material propensities is considered. To solve the governing equation for FG disks, one-dimensional second (two) degree elements with three nodes are used. The temperature distribution is as second order variation, while the material properties vary using a power law function in the radial direction of the disk.

Validation and convergence is checked and good agreement is observed with other literature. The numerical example in model-A (thermal stress) shows that the displacements and stresses increased by increasing power law index N and the angular velocity. Modeling of the dependency and independency of the material properties on the temperature proves a significant discrepancy in the results, which should be considered in design procedures. In another numerical example in model-B (mechanical stress), it has been shown that different types of profile surfaces of FG disk have different complex behaviors due to the distribution of material properties.

References

[1] S. Suresh and A. Mortensen, *Fundamental of functionally graded materials*, Barnes and Noble Publication (1998).

[2] L. H. You, J. X. Wang and B. P. Tang, Deformations and stresses in annular disks made of functionally graded materials subjected to internal and/or external pressure, *Meccanica*, 44 (2009) 283-292.

[3] M. Koizumi and M. Niino, Overview of FGM research in Japan, *MRS Bulletin*, 20 (1995) 19-21.

[4] W. A. Kaysser and B. Ilschner, FGM research activities in Europe, *MRS Bulletin*, 20 (1995) 22-26.

[5] Research on the basic technology for the development of functionally graded materials for relaxation of thermal stress, Science on Technology Agency of Japanese Government Report (1987).

[6] S. P. Timoshenko and J. N. Goodier, *Theory of elasticity*, McGraw-Hill, New York (1987).

[7] S. G. Lekhnitskii, *Anisotropic plates*, Gordon and Breach, London (1968).

[8] A. Seireg and K. S. Surana, Optimum design of rotating disks, *Journal of Engineering*, 92 (1970) 1-10.

[9] D. N. S. Murthy and A. N. Sherbourne, Elastic stresses in anisotropic disks of variable axial, *Journal of Mechanical Science*, 12 (1970) 627-640.

[10] K. Y. Yeh and R. P. S. Han, Analysis of high-speed rotating disks with variable axial and in-homogeneity, *Journal of Applied Mechanics*, 61 (1994) 186-191.

[11] M. Azadi and M. Azadi, Nonlinear transient heat transfer and thermoelastic analysis of thick-walled FGM cylinder with temperature-dependent material properties using Hermitian transfinite element, *Journal of Mechanical Science and Technology*, 23 (2009) 2635-2644.

[12] M. Azadi and M. Shariyat, Nonlinear transient transfinite element thermal analysis of thick-walled FGM cylinders with temperature-dependent material properties, *Meccanica*, 45:3 (2010) 305-318, DOI: 10.1007/s11012-009-9249-4.

[13] M. Azadi and M. Damircheli, Nonlinear thermoelastic stress analysis of the rotating FGM disks with variable thickness and temperature-dependent material properties using finite element method, *Proceeding of the 14-th International Conference on Mechanical Engineering*, No. IMECE2009-12204, Lake Buena Vista, Florid, USA (2009).

[14] A. W. Leissa and M. Vagins, The design of orthotropic materials for stress optimization, *Journal of Solids Structures*, 14 (1987) 517-526.

[15] R. Jain, K. Ramachandra and K. R. Y. Simha, Rotating anisotropic disc of uniform strength, *Journal of Mechanical Science*, 41 (1999) 639-648.

[16] R. Jain, K. Ramachandra and K. R. Y. Simha, Singularity in rotating orthotropic discs and shells, *Journal of Solids Structures*, 37 (2000) 2035-2058.

[17] F. Zhou and A. Ogawa, Elastic solutions for a solid rotating disk with cubic anisotropy, *Journal of Applied Mechanics*, 69 (2002) 81-83.

[18] S. A. Ramu and K. J. Iyengar, Quasi-three dimensional elastic stresses in rotating disks, *Journal of Mechanical Science*, 16 (1974) 473-477.

[19] W. Q. Chen and K. Y. Lee, Stresses in rotating cross-ply laminated hollow cylinders with arbitrary axial, *Journal of Strain Analysis*, 39 (2004) 437-445.

[20] M. A. Mian and A. J. M. Spencer, Exact solutions for functionally graded and laminated elastic materials, *Journal of Solid Mechanics*, 46 (1998) 2283-2295.

[21] J. Chen, H. Ding and W. Chen, Three-dimensional analytical solution for a rotating disc of functionally graded materials with transverse isotropy, *Journal of Applied Mechanics*, 77 (2007) 241-251.

[22] A. M. Zenkour, Stress distribution in rotating composite structures of functionally graded solid disks, *Journal of Materials Processing Technology* (2008), DOI: 10.1016/ j.jmatprotec.2008.08.008.

[23] M. Bayat, M. Saleem, B. B. Sahari, A. M. S. Hamouda and E. Mahdi, Analysis of functionally graded rotating disks with variable thickness, *Mechanics Research Communications*, 35 (2008) 283-309.

[24] M. Bayat, B. B. Sahari, M. Saleem, A. Ali and S. V. Wong, Thermoelastic solution of a functionally graded variable thickness rotating disk with bending based on the first-order sheared formation theory, *Journal of Thin-Walled Structures* (2008), DOI: 10.1016/j.tws.2008.10.002.

[25] J. Chen, H. Ding and W. Chen, Three-dimensional analytical solution for a rotating disc of functionally graded materials with transverse isotropy, *Archive of Applied Mechanics*, 77 (2007) 241-251.

[26] J. N. Reddy and C. D. Chin, Thermo-mechanical analysis of functionally graded cylinders and plates, *Journal of Thermal Stresses*, 21 (1998) 593-626.

[27] R. G. Budynas, *Advanced Strength and Applied Stress Analysis*, McGraw-Hill Kogakusha, Ltd., Tokyo (1977).

[28] T. J. R. Hughes, *The finite element method*, Prentice-Hall International Inc. (1987).

[29] J. N. Reddy, *An introduction to the finite element method*, McGraw-Hill Institute (1993).

[30] A. P. Boresi and K. P. Chong, *Elasticity in engineering mechanics*, second edition, A Wily-Interscience publication (2000).

Mehrnoosh Damircheli received her B.S. in Mechanical Engineering from Kerman University (shahid bahonar), Iran, in 1999. She then earned her M.S. from Islamic Azad University South Tehran Branch in 2002. She is currently a Ph.D candidate at Islamic Azad University science and research branch in Tehran. Her research interests include Nano Robotic, AFM (atomic force microscoe), Composites (especially FGMs), FEM (Finite Element Method), Vibration and effects of higher hamonics exicitation, chaotic and control.

Mohammad Azadi received his B.S. in Mechanical Engineering from Shiraz University, Iran, in 2006. He then received his M.S. from K.N. Toosi University of Technology in 2008. He is currently a Ph.D candidate at Sharif University of Technology. His research interests include NVH (Noise, Vibration and Harshness), Composites (especially FGMs), FEM (Finite Element Method), automotive engineering (especially engines and vehicle structure), TBC (Thermal Barrier Coating) and fatigue including HCF (High Cycle Fatigue), LCF (Low Cycle Fatigue) and TMF (Thermo-Mechanical Fatigue).